

Laser-induced reentrant freezing in two-dimensional attractive colloidal systems

Pinaki Chaudhuri,^{1,2} Chinmay Das,³ Chandan Dasgupta,^{1,2} H. R. Krishnamurthy,^{1,2} and A. K. Sood^{1,2}

¹Department of Physics, Indian Institute of Science, Bangalore, India

²Jawaharlal Nehru Centre for Advanced Scientific Research, Bangalore, India

³Department of Applied Mathematics, University of Leeds, Leeds, United Kingdom

(Received 7 September 2005; published 20 December 2005)

The effects of an externally applied one-dimensional periodic potential on the freezing and melting behavior of two-dimensional systems of colloidal particles with a short-range attractive interaction are studied using Monte Carlo simulations. In such systems, incommensuration results when the periodicity of the external potential does not match the length scale at which the minimum of the attractive potential occurs. To study the effects of this incommensuration, we consider two different models for the system. Our simulations for both these models show the phenomenon of reentrant freezing as the strength of the periodic potential is varied. Our simulations also show that different exotic phases can form when the strength of the periodic potential is high, depending on the length scale at which the minimum of the attractive pair potential occurs.

DOI: [10.1103/PhysRevE.72.061404](https://doi.org/10.1103/PhysRevE.72.061404)

PACS number(s): 82.70.Dd, 64.70.Dv

I. INTRODUCTION

In the pioneering experiments of Chowdhury, Ackerson, and Clark [1] on laser induced freezing, a two-dimensional monolayer of colloidal particles in the liquid state was subjected to a laser intensity pattern periodically modulated along one direction. They found that if the wave vector of the modulation is tuned to the wave vector at which the liquid structure factor peaks, a triangular lattice with full two-dimensional symmetry results for laser intensities above a threshold value. In a later experiment Wei *et al.* [2] observed that this triangular lattice melts if the strength of the laser field is increased further. Although such a “reentrant melting” phenomenon was observed in Monte Carlo studies [3] of colloidal particles interacting via Derjaguin-Landau-Verwey-Overbeek (DLVO) [4] potential, later simulations of the same system by Das *et al.* [5] did not show the reentrant phase. However, by extending the Kosterlitz-Thouless-Halperin-Nelson-Young [6] theory of defect-mediated melting in two dimensions to the case where an external periodic potential is present, Frey *et al.* [7] argued that for short-range interactions there will indeed be a reentrant transition to a liquid state. Later experiments [8] and simulations [9] of charged colloids seem to confirm the occurrence of reentrant melting. Meanwhile, numerical studies [10,11] of the effect of the external periodic potential on a system of hard disks have also shown the occurrence of reentrant melting.

All the above results correspond to the case when the commensurability ratio $p = \sqrt{3}a/2d$ (where a is the mean particle distance and d is the period of the external periodic potential) has the value of 1, i.e., every potential trough is occupied by particles. In a recent experiment [12] corresponding to $p=2$, a new phase—the “locked smectic state”—was observed, with the crystalline state being found to melt via this new intermediate phase. This observation is also in qualitative agreement with theoretical predictions [7].

No study has been reported as yet for the case where there is a possibility of incommensuration between the periodicity of the external laser field and some length scale inherent to

the two-dimensional colloidal system. In the present work we study just such a case. Specifically, we look at the effect of the external laser field on a monolayer of colloidal particles, which interact via a short-range attraction apart from the usual hard-core repulsive interaction. Such a short-range attraction is known to arise when hard sphere colloidal particles are mixed with polymers or smaller colloidal particles, giving rise to an effective attraction [13] between the larger particles, called depletion interaction. It has also been suggested in the context of colloidal particles confined between two walls [14,15], where it is claimed that an attractive minimum in the effective interaction between a pair of colloidal particles arises when they are close to the walls [16]. Effects due to incommensuration should occur if the length scale at which the attractive part of the interaction has its minimum is different from the periodicity of the externally applied laser field. Novel phases can then appear in the system depend-

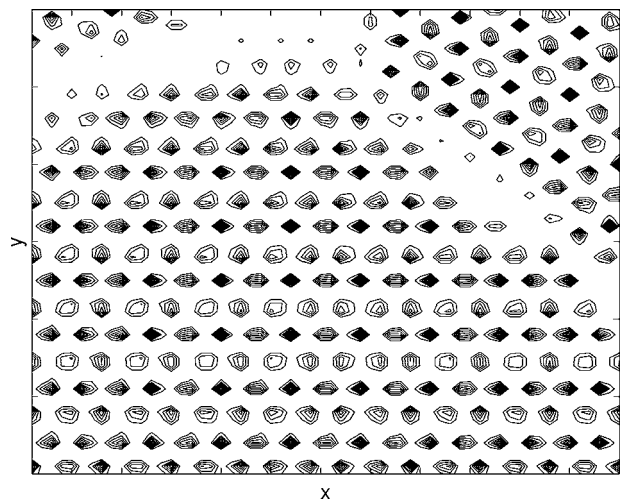


FIG. 1. Model 1. Average particle density $\rho(x, y)$ at $\bar{\rho}=0.86$, for the case when the external field is absent, showing coexistence of crystalline clusters with a gaseous phase. The average density is shown for a section of size 17.38σ in the x direction and $17.38(\sqrt{3}/2)\sigma$ in the y direction.

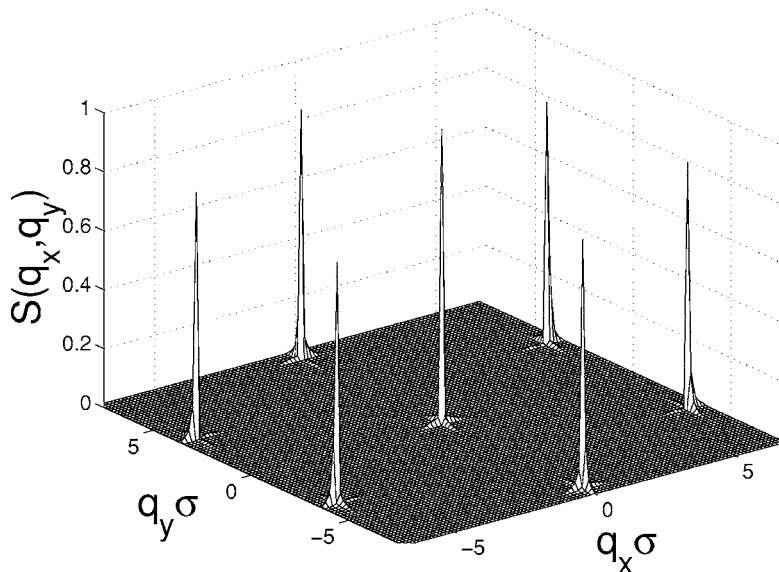


FIG. 2. Model 1. Structure factor $S(\mathbf{q})$ of a colloidal cluster at $\bar{\rho}=0.86$, for the case when the external field is absent, showing the existence of triangular lattice structure within the cluster.

ing upon the relative strengths of the two competing potentials with different length scales.

Recently, Götze *et al.* [17] studied the effect of an external potential with one-dimensional periodic modulation on the liquid-vapor transition line of a three-dimensional mixture of hard-sphere colloidal particles and polymers. In their density functional calculations, they obtained a new *stacked fluid* phase, which consists of a periodic succession of liquid and vapor slabs. The presence of this new phase is a manifestation of the one-dimensional nature of the externally applied modulated potential in a three-dimensional fluid. Their simulations and calculations also showed that the density profiles exhibit a nonmonotonic crossover when the wavelength of the modulation matches the hard sphere diameter.

In the present work, we analyze the effects of incommensuration on the phenomenon of freezing and melting of colloidal particles in two dimensions in the presence of a tunable “substrate” or external potential with one-dimensional periodic modulation. For this purpose, we consider two different models that are described in Sec. II, and use Monte Carlo simulations to study their behavior. In our simulations of these two models, we clearly see that for both low and high values of the external potential the colloidal particles form crystalline structures, whereas for intermediate strengths of the external potential the system is in a modulated liquid phase. We term this phenomenon *reentrant freezing*. It is also observed that at high values of the external potential, different kinds of phases can occur depending on

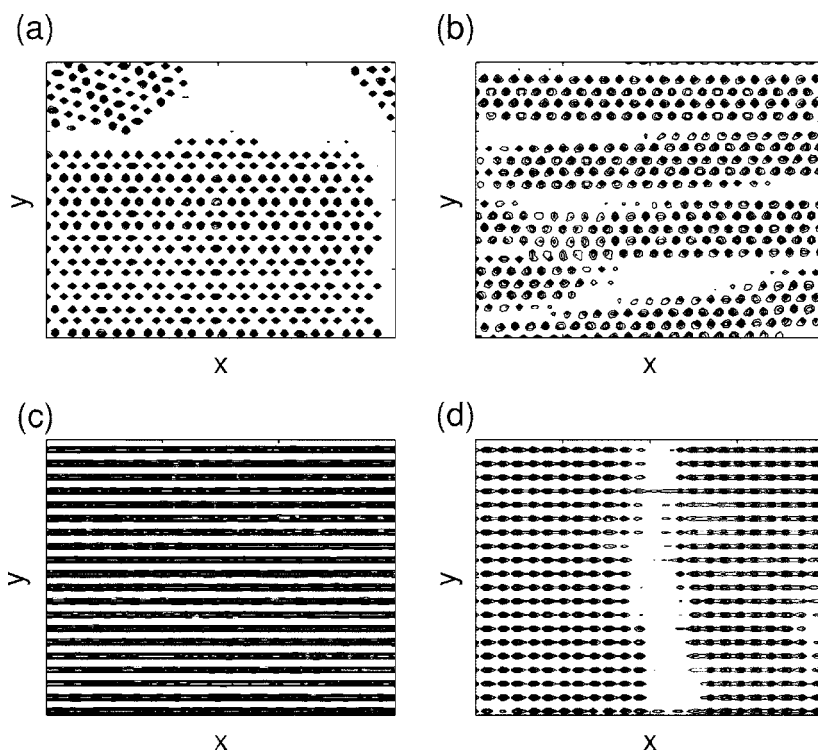


FIG. 3. Model 1. At $\bar{\rho}=0.86$, the average particle density $\rho(x,y)$ shows (a) a two-dimensional (2D) triangular lattice when $\beta V_e=0.5$, (b) a “frustrated” liquid when $\beta V_e=2.0$, (c) a modulated liquid when $\beta V_e=5.0$, and (d) a 2D square lattice $\beta V_e=100.0$. Thus, at this density, the system undergoes reentrant freezing as a function of the strength of the externally applied field. In each of the plots, $\rho(x,y)$ is shown for a section of size 23.18σ in the x direction and $23.18(\sqrt{3}/2)\sigma$ in the y direction.

the length scale at which the attractive part of the interparticle potential has its minimum. Our simulation results are described in detail in Sec. III. The main conclusions of this study are summarized in Sec. IV.

II. THE MODELS

A. Hard-core particles with short-range attraction

The generation of an effective attractive interaction between large hard-sphere colloid particles when they are

$$U(r_{ij}) = \begin{cases} \infty & \text{if } r_{ij} < \sigma, \\ -\mathcal{U} \left[\cos^{-1} \left(\frac{\eta r_{ij}}{1 + \eta \sigma} \right) - \left(\frac{\eta r_{ij}}{1 + \eta \sigma} \right) \sqrt{1 - \left(\frac{\eta r_{ij}}{1 + \eta \sigma} \right)^2} \right] & \text{if } \sigma \leq r_{ij} \leq \sigma \left(1 + \frac{1}{\eta} \right), \\ 0 & \text{if } r_{ij} > \sigma \left(1 + \frac{1}{\eta} \right). \end{cases} \quad (2.1)$$

Here, σ is the particle diameter and \mathcal{U} and η are two parameters which can be used to tune the depth and width of the short-range attractive part of $U(r_{ij})$. This interaction potential has a minimum at $r_{ij} = \sigma$, i.e., when the two particles touch each other. The strength of the interaction potential at this minimum is given by

$$U_{\min} = \mathcal{U} \left[\cos^{-1} \left(\frac{\eta}{1 + \eta} \right) - \left(\frac{\eta}{1 + \eta} \right) \sqrt{1 - \left(\frac{\eta}{1 + \eta} \right)^2} \right]. \quad (2.2)$$

In addition, we assume that a particle with coordinates (x, y) experiences an external periodic potential of the form

$$V(x, y) = V_e \cos \left(\frac{2\pi}{d} y \right). \quad (2.3)$$

In the above equation, the constant d is chosen such that for a number density of $\phi = N/(L_x L_y)$ (N is the number of particles and L_x, L_y are the lengths of the sides of a rectangular sample), the modulation is commensurate with a triangular lattice with nearest neighbour distance $a_s = 1/[(\sqrt{3}/2)\phi]^{1/2}$, i.e., $d = a_s \sqrt{3}/2$. Thus, for the binary mixture we are trying to model, the wave vector of the external potential is commensurate with the smallest reciprocal lattice vector [$q_0 = 2\pi/(a_s \sqrt{3}/2)$] of the triangular lattice that the large disks would form at that density in the absence of the smaller disks. Also, the form of the external potential is such that its troughs run parallel to the x axis.

For the system under study, the important parameters are $U_0 = \beta U_{\min}$, βV_e , $\bar{\rho} = \phi \sigma^2$, and η , where $\beta = 1/(k_B T)$, k_B being the Boltzmann constant and T the temperature. While the attractive part of $U(r_{ij})$ would like to have the particles touching each other (with interparticle separation σ), the

externally applied potential would like to have a density modulation in the \hat{y} direction with periodicity d , resulting in the incommensuration.

B. Soft-core particles with short-range attraction

The second model we consider is one where the attractive potential is considered to be a Gaussian well, with the position of its minimum being incommensurate with the interparticle separation. Thus, the pair potential $U(r_{ij})$ between particles i and j with distance r_{ij} is given by

$$U(r_{ij}) = \frac{1}{2} \left[\frac{(Z^* e)^2}{\epsilon} \left(\frac{\exp(\kappa R)}{1 + \kappa R} \right)^2 \frac{\exp(-\kappa r_{ij})}{r_{ij}} - A \exp[-B(r_{ij} - \Lambda)^2] \right], \quad (2.4)$$

where R is the radius of the colloidal particles with surface charge $Z^* e$ and κ is the inverse of the Debye screening length. Similarly to the first model, in this case also a colloidal particle with coordinates (x, y) is assumed to experience an external periodic potential of the form

$$V(x, y) = V_e \cos \left(\frac{2\pi}{d} y \right). \quad (2.5)$$

As in the first model, the modulation of the external potential d is chosen such that for colloidal particles with density $\phi = N/(L_x L_y)$, the modulation is commensurate with a triangular lattice with nearest neighbor distance $a_s = 1/[(\sqrt{3}/2)\phi]^{1/2}$, i.e., $d = a_s \sqrt{3}/2$. The parameter Λ in Eq. (2.4), which determines the position of the minimum of the attractive part of the potential, is assumed to be incommensurate with the triangular lattice. The parameter A determines the depth of the attractive well and B determines its width.

This model was motivated in part by the suggestion [14,15] that in a two-dimensional monolayer of charged col-

loidal particles in an aqueous solution confined between two walls, with the “bare” interaction between pairs of particles being given by the Derjaguin-Landau-Verwey-Overbeek potential [4], an attractive well with a depth of the order of $k_B T$ develops in the *effective potential* between a pair when the particles are near a charged wall. The depth and the position of the minimum are supposed to be strongly dependent on the distance from the wall, the effective charge on the colloid particles, the counter-ion density and the surface charge on the wall. However, this claim has been contested [16]. In any case, leaving aside the question of a physical realization of the above model, its use tests the robustness of our results with respect to the details of the model interaction.

III. SIMULATIONAL DETAILS AND RESULTS

A. Model 1

We have carried out Monte Carlo simulations of a system of N particles of diameter σ , interacting via the potential $U(r_{ij})$ defined in Eq. (2.1). The particles are contained in a rectangular box of dimension $L_x \times L_y$, where $(L_y/L_x = \sqrt{3}/2)$, with periodic boundary conditions being used for doing the Monte Carlo simulations. Most results reported here are for simulations done for $N=1600$ particles. In order to check

finite size effects, we will also discuss results for $N=1024$ and 900.

For a system of particles interacting via the potential specified in Eq. (2.1), the phase diagram is not known even when the external laser field is absent. However, Brownian dynamics simulations for a similar system [19] suggest that at $U_0 \approx 3.1$, there is a transition from a single, dispersed phase to a phase where the colloidal particles start forming clusters. In our present work, we consider the case $U_0=5.4$ and $\eta=30$. The first parameter defines the depth of the attractive potential and the second one fixes its width ($\sigma/30$). In the range of densities of our interest, $0.85 < \bar{\rho} < 0.95$, Bolhuis *et al.* [20] have observed the co-existence of a high-density solid with a dilute gas for a two-dimensional system of particles interacting via a short-range attractive square potential. Coexisting gas and solid phases are also found in three dimensions [21] when the interparticle attraction has a short range. Our simulations also show the formation of clusters for the choice of U_0 and η mentioned above. In Fig. 1, we have plotted the average density, representative of our simulated system, at $\bar{\rho}=0.86$. The plot clearly shows the co-existence of crystalline clusters with a gaseous phase, with particles arranged in a triangular lattice inside the clusters, as observed in the Brownian dynamics simulations [19]. The structure factor $S(\mathbf{q})$ for a cluster, plotted in Fig. 2, shows peaks corresponding to a triangular lattice structure with

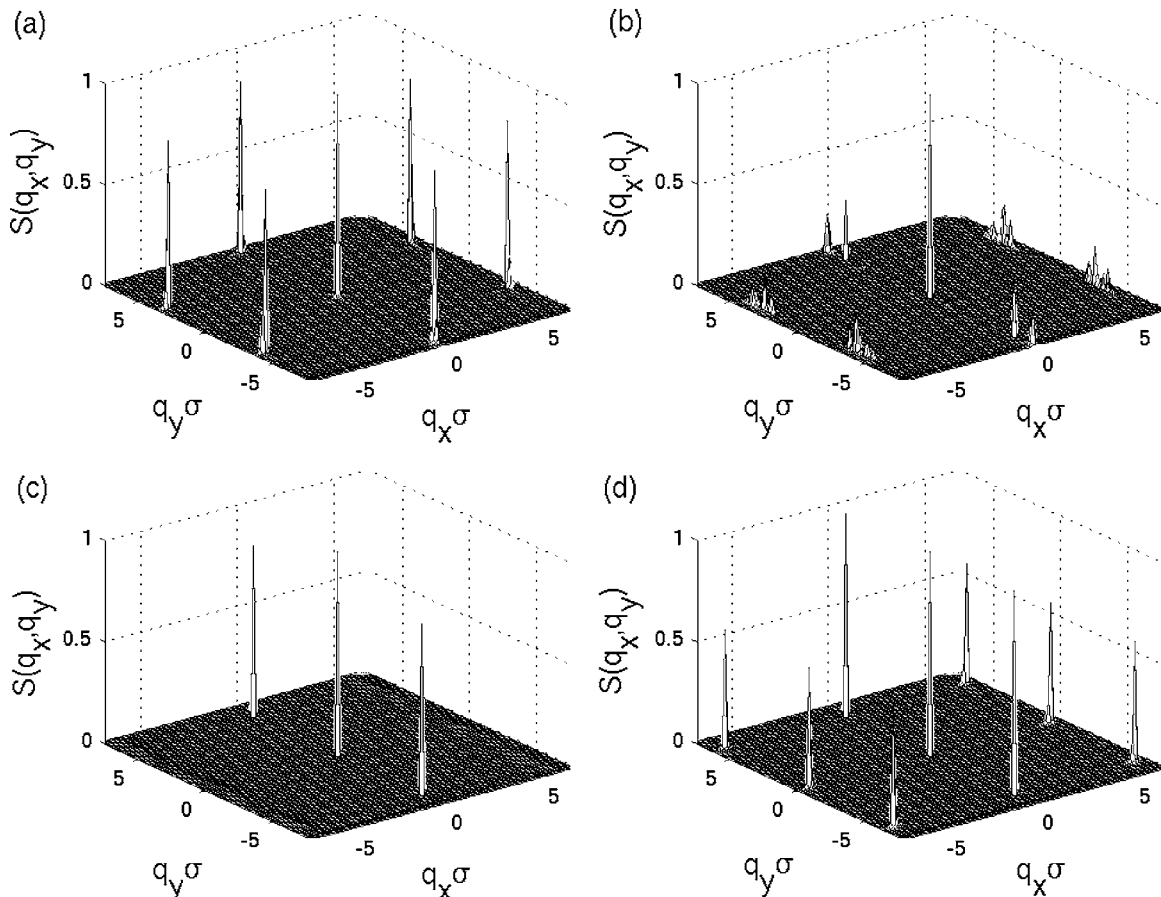


FIG. 4. Model 1. For $\bar{\rho}=0.86$, structure factor $S(\mathbf{q})$ shows (a) a 2D triangular lattice when $\beta V_e=0.5$, (b) a “frustrated” liquid when $\beta V_e=2.0$, (c) a modulated liquid when $\beta V_e=5.0$, (d) a 2D square lattice when $\beta V_e=100.0$, confirming the reentrant freezing experienced by the system as βV_e is increased.

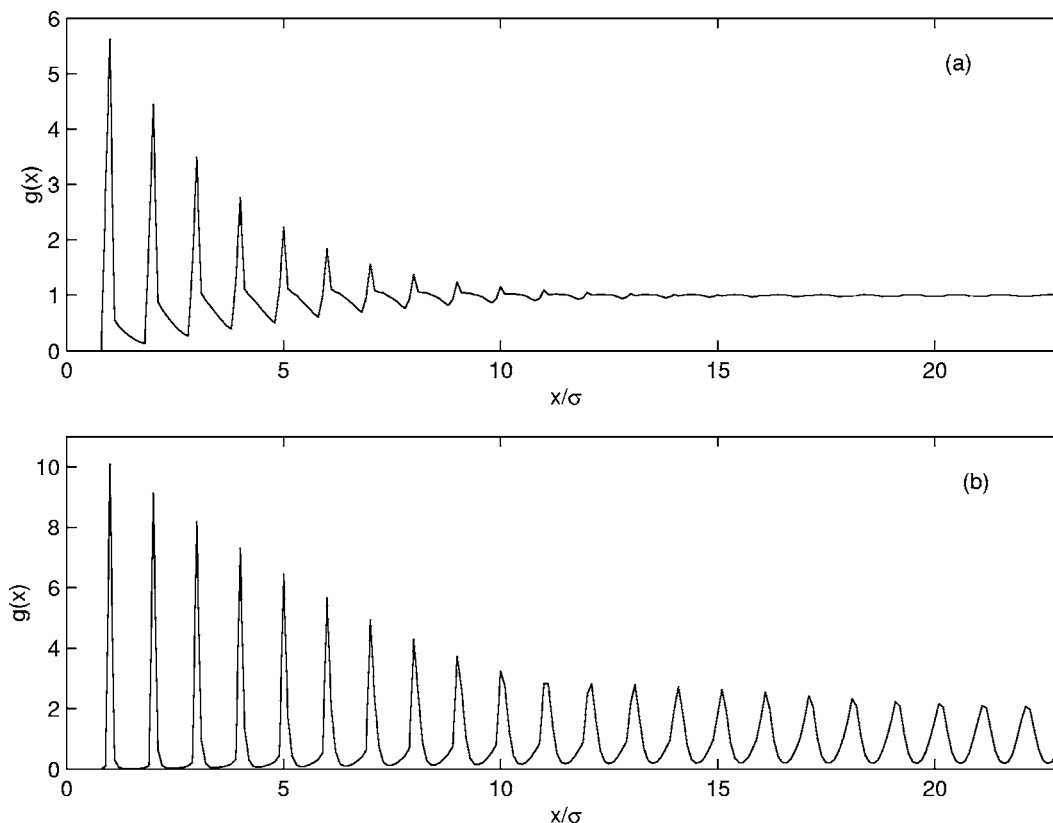


FIG. 5. Model 1. Pair correlation functions $g(x)$, at $\bar{\rho}=0.86$, along the potential troughs for (a) a modulated liquid (when $\beta V_e=5$) and (b) a square lattice (when $\beta V_e=100$).

spacing equal to σ , the hard-sphere diameter.

Our objective is to study how such a system of colloidal particles behaves in the presence of an external potential with one-dimensional periodic modulation d which is not commensurate with the distance between the lattice planes of the triangular structure that the particles form in the absence of the field. For this purpose we calculate the average density $\rho(x, y)$ and the structure factor $S(\mathbf{q})$ for different strengths of the potential at a fixed particle density.

For $\bar{\rho}=0.86$, when the strength of the potential is low, our simulations show that the system continues to form crystalline clusters with interparticle separation σ . In Figs. 3(a) and 4(a), we have plotted, respectively, the average density and the corresponding $S(\mathbf{q})$ for the colloidal system when the strength of the laser-induced potential is $\beta V_e=0.50$. As can be seen from the plots, the nature of $S(\mathbf{q})$ is similar to the case where the potential is absent.

When the strength of the potential is increased to $\beta V_e=2.0$, the clusters break up and the particles try to align themselves along the potential troughs. The average density $\rho(x, y)$ for this value of βV_e , plotted in Fig. 3(b), shows that although there is a local triangular structure, the particles are also getting arranged in the \hat{y} direction, due to the influence of the external potential. The $S(\mathbf{q})$ for this situation, plotted in Fig. 4(b), shows that the height of the peaks corresponding to the triangular lattice has decreased considerably compared to that in Fig. 4(a) and new peaks have begun to appear on the \hat{q}_y axis with q_y values corresponding to the wave vector of the applied field. This clearly is an effect of the incom-

mensuration. The system is in a “frustrated” state—the particles are making an attempt to lie at the troughs of the periodic potential, but the energy they gain by doing so is not sufficient to break the “bonds” of the triangular lattice with spacing σ .

In Fig. 3(c), we have plotted $\rho(x, y)$ for the system when the strength of the laser field has been increased to $\beta V_e=5.0$. The crystalline clusters have now melted—the particles have become confined along the potential troughs. The $S(\mathbf{q})$ for the system, plotted in Fig. 4(c), is characteristic of a modulated liquid, with the peaks of the structure factor located only at multiples of the characteristic wave vector $q_y=2\pi/d$ of the external periodic potential.

When the strength of the periodic potential is increased to higher values, the motion of the particles in the direction transverse to the potential troughs decreases considerably. The average density for the particles at a potential strength of $\beta V_e=100.0$, plotted in Fig. 3(d), shows crystalline order corresponding to a square lattice, which is also reflected in the corresponding $S(\mathbf{q})$, shown in Fig. 4(d). The peaks of the structure factor on the \hat{q}_y axis occur at wave vectors that correspond to multiples of the wave vector of the external potential, whereas the peaks on the \hat{q}_x axis correspond to an interparticle separation of σ inside each potential trough.

We have also computed the spatial correlation function $g(x)$, which is the pair correlation function along the potential troughs, for the two phases observed for the potential strengths $\beta V_e=5.0$ and 100.0 . The maxima of the correlation function for $\beta V_e=5.0$, plotted in Fig. 5(a), decay quite fast,

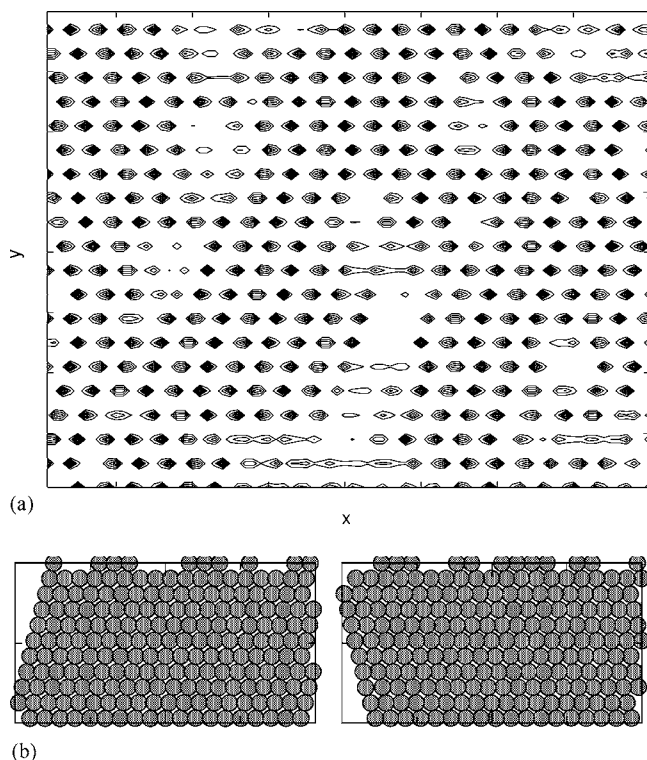


FIG. 6. Model 1. (a) The average density for $\bar{\rho}=0.92$ at $\beta V_e=100$, showing that the particles form a mixed crystal. The plotted average density is for a section of size 22.40σ in the x direction and $22.40(\sqrt{3}/2)\sigma$ in the y direction. (b) The two panels are snapshots of the crystalline structures having the same energy, one of which will be formed by the particles as $\beta V_e \rightarrow \infty$, at $\bar{\rho}=0.92$.

and at long distances $g(x) \rightarrow 1$. This is characteristic of liquidlike behavior for the particles confined in the potential troughs. However, when $\beta V_e=100.0$, from the $g(x)$ data plotted in Fig. 5(b), we can conclude that there is a periodic modulation of the density of the colloidal particle in the potential troughs, the period of this modulation being σ as expected.

To check whether the formation of the crystalline solid at the higher values of βV_e is a finite size effect, we have calculated the corresponding order parameter $\rho_{\mathbf{q}}$ for different system sizes, $N=1600, 1024, 900$. For the solid phase, the order parameters are the Fourier components of the density $\rho(\mathbf{r})$ calculated at the reciprocal lattice points $\{\mathbf{q}\}$. From the peaks of the structure factor plotted in Fig. 4(d), we can get the four smallest reciprocal lattice vectors for the square lattice formed by the particles for $\beta V_e=100.0$. Of these four vectors, the two lying on the $\hat{\mathbf{q}}_y$ axis correspond to the ordering due to the external field and the $\rho_{\mathbf{q}}$ for these vectors are also nonzero for the modulated liquid. So the $\rho_{\mathbf{q}}$ for the other two wave vectors, denoted by $\rho_{\mathbf{q}}^\perp$, are the relevant order parameters for checking the effects of the finiteness of the system. The average order parameter $\langle \rho_{\mathbf{q}}^\perp \rangle$ has the values 0.731, 0.663, 0.661 for $N=900, 1024, 1600$, respectively, implying weak dependence on the system size. Therefore, we can conclude that the square lattice formed at $\beta V_e=100.0$ represents a crystalline phase.

The appearance of this crystalline phase at a large value

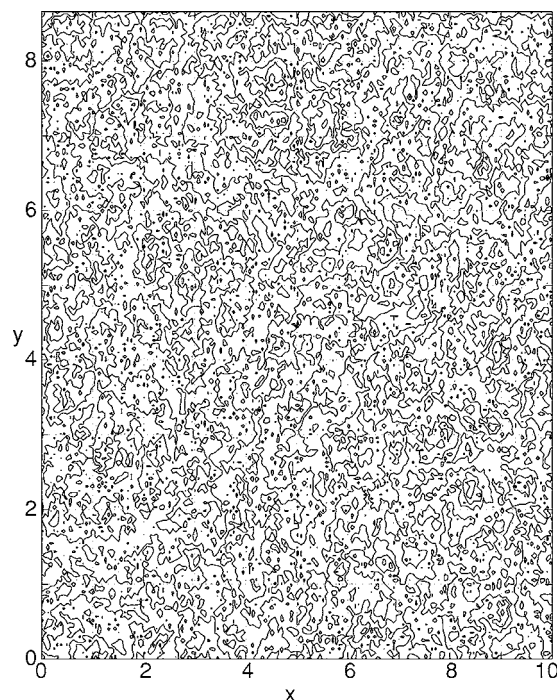


FIG. 7. Model 2. Average density $\rho(x,y)$ in the absence of an external field and attractive potential for $\kappa a_s=15$.

of βV_e can be understood from the fact that, for $\bar{\rho}=0.86$, the intertrough spacing, which is governed by the periodicity of the external field d , is approximately equal to σ , the distance at which $U(r_{ij})$ has its minimum. In fact, for $0.811 \leq \bar{\rho} \leq 0.866$, the spacing d is within the range of the attractive part of the potential, $1.033 \leq r/\sigma \leq 1.0$, for the value of η used in our simulations. Thus, at $\bar{\rho}=0.86$, if the transverse motion within a trough is suppressed, correlations develop across the troughs resulting in ordering of the particles in the $\hat{\mathbf{y}}$ direction, in addition to the ordering with spacing σ along the troughs. Such a crystal structure corresponds to the lowest energy configuration consistent with the density and the intertrough spacing.

Thus the system of colloidal particles, which had preferred to form crystalline clusters at low field strengths, regains a different crystalline phase at high field strengths, after passing through an intermediate modulated liquid phase. This phenomenon may be called *reentrant freezing*. It is interesting to note that the two crystalline phases have different symmetries, which is a consequence of the incommensuration effects. Another aspect to note is that the solid is in coexistence with a dilute gas and the “voids” corresponding to the gaseous phase can occur at any point in space. This is a probable reason for the decrease in the height of the maxima of $g(x)$ at large distances. The intertrough correlations, observed at $\beta V_e=100.0$, are not developed at lower field strengths because the motion of the particles in the transverse direction is not suppressed sufficiently and the particles can vibrate within the width provided by the trough, thereby causing a destruction of the crystalline order.

However, we should note that the kinetics of systems with hard-core interactions may depend strongly on the initial state [21]. In our simulations, we observe such behavior. For

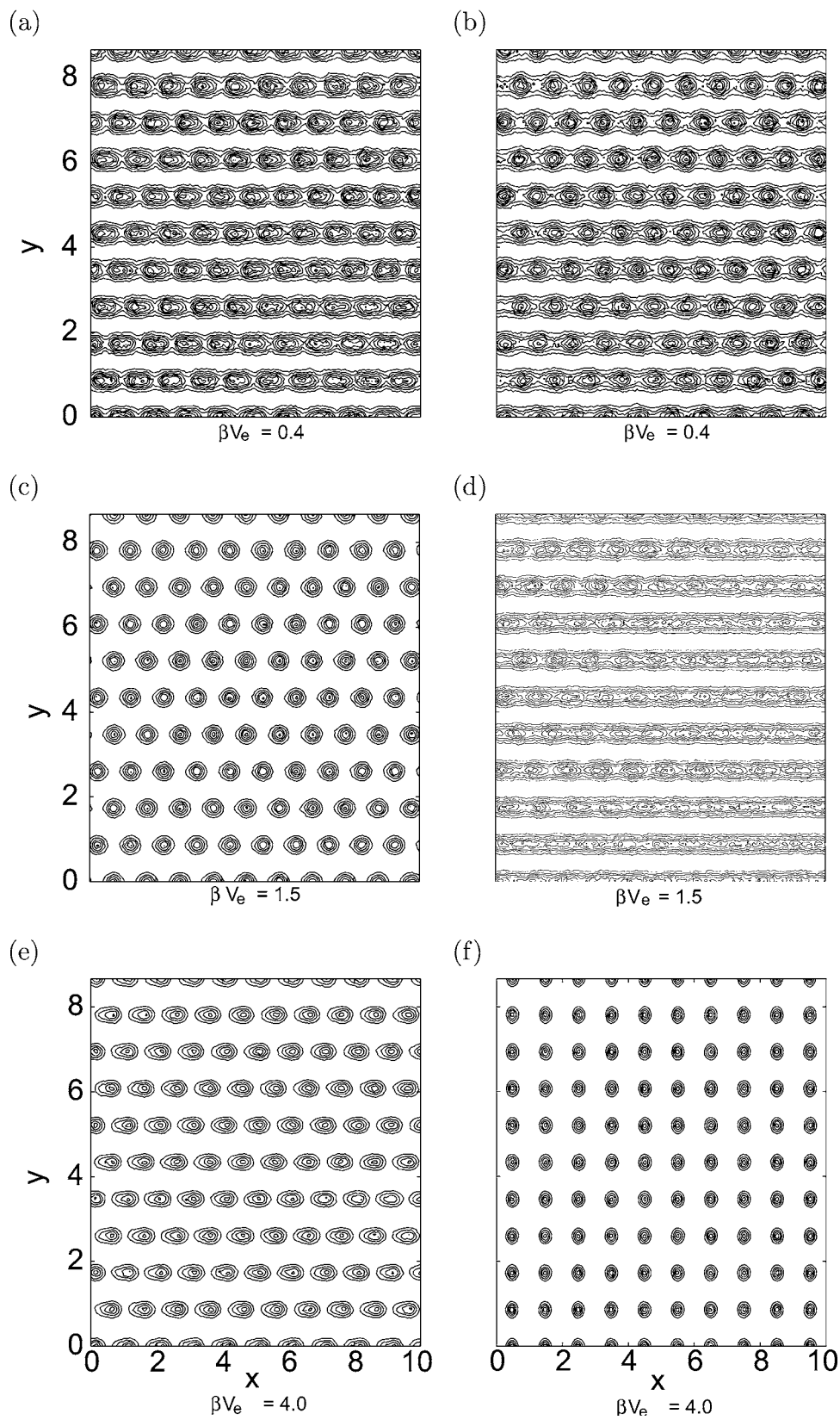


FIG. 8. Model 2. The left hand panels (a), (c), and (e) show the average density for simulations with just the DLVO potential. The right hand panels (b), (d), and (f) show the same for simulations with an attractive potential.

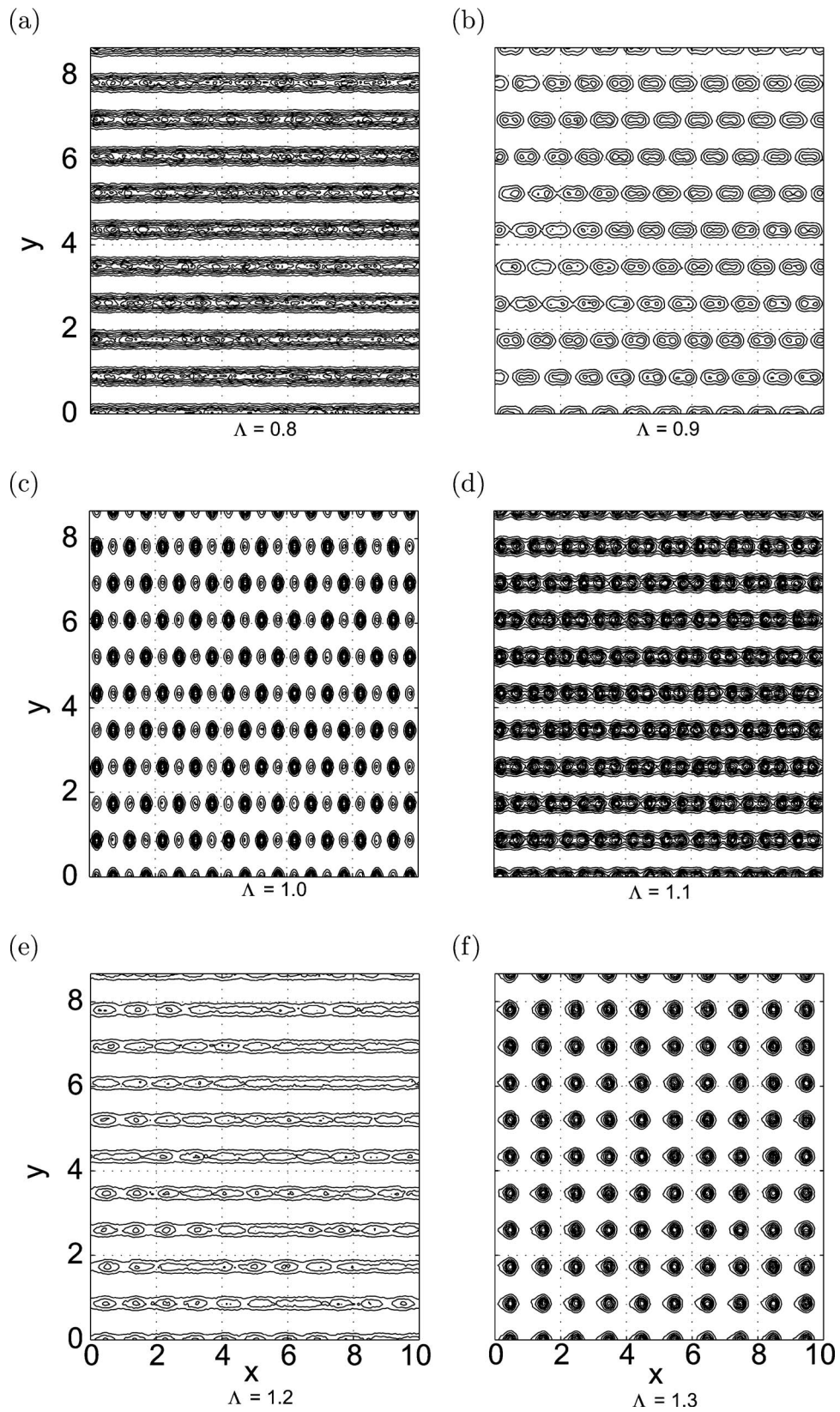


FIG. 9. Model 2. Average density for $\kappa a_s=15$, $\beta V_e=4$, and with different values of Λ .

some initial configurations, the system gets kinetically jammed and due to this jamming, even at high field strengths, there is a coexistence of the square and triangular

phases. In simulations, one can escape from jamming if a combination of local and nonlocal Monte Carlo moves are used.

For $\bar{\rho} > 0.866$, the wavelength of the external potential becomes smaller than the particle diameter and therefore, for these densities, the square lattice become unfeasible at high potential strengths. However, even for these densities, the particles in neighboring troughs would like to be in contact with each other and that can only happen if they form a rhombic structure. In Fig. 6, we have plotted the average density for $\bar{\rho} = 0.92$ at $\beta V_e = 100.0$. The particles have formed a “mixed crystal,” i.e., they have formed domains which have local crystalline structure similar to the two structures shown in the figures below the $\rho(x, y)$ plot. As $\beta V_e \rightarrow \infty$, the motion of the particles becomes one dimensional and the system tries to attain one of these two crystalline structures in order to minimize its free energy.

B. Model 2

For the other choice of the pair potential given in Eq. (2.4), we have considered 400 particles in a rectangular box commensurate with a triangular lattice structure and with periodic boundary conditions. The screening length is fixed at $\kappa a_s = 15.0$ where a_s , the lattice spacing in a triangular arrangement, has been used as the unit of length in all the expressions. Without any external field, the system (colloidal particles of diameter $1.07 \mu\text{m}$, surface charge $Z^* = 7800e$, and density $n_p = 1.81 \times 10^7/\text{cm}^2$, suspended in water having dielectric constant $\epsilon = 78$ at a room temperature of 298 K) is in the liquid phase. The parameters for the Gaussian well are chosen as $A = V_e/2$ and $B = 50$. In the first part of our simulations for this system, the position of the attractive minimum is set at $\Lambda = 1.3$.

To observe the effect of the laser field in this system of particles, the average density is calculated for different values of βV_e . In Fig. 7, we have shown a contour plot of the average density, representing a section of the simulation box, in the absence of the external potential. The average density does not show any order, signifying a liquid state.

Figure 8 contrasts the effect the external potential has on the average density depending on whether the interparticle potential has the attractive part or not. At $\beta V_e = 0.4$ [subplots (a) and (b)], the liquidlike structure of Fig. 7 is replaced by one corresponding to a triangular lattice structure in both cases. The order parameter ρ_q^\perp , corresponding to the triangular lattice structure, has the value 0.6 for the pure DLVO potential and 0.53 for the case when the attractive part is present. As the field is increased to $\beta V_e = 1.5$, the crystalline order for the pure DLVO potential becomes much sharper [see Fig. 8(c)], and the value of ρ_q^\perp (for the triangular lattice) becomes higher. But with the attractive part present [see Fig. 8(d)], the average density looks like a set of liquidlike strings, indicating a modulated liquid phase, with ρ_q^\perp (for the triangular lattice) becoming much smaller ≈ 0.15 . At still higher fields, $\beta V_e = 4.0$, nothing changes qualitatively for the pure DLVO case [see Fig. 8(e)]. However, the average density plot for the case with the attractive potential [Fig. 8(f)] indicates the formation of a rectangular lattice.

Therefore, for this choice of interparticle potential, we again find that the system of colloidal particles, which had formed a crystalline structure for low strength of the external

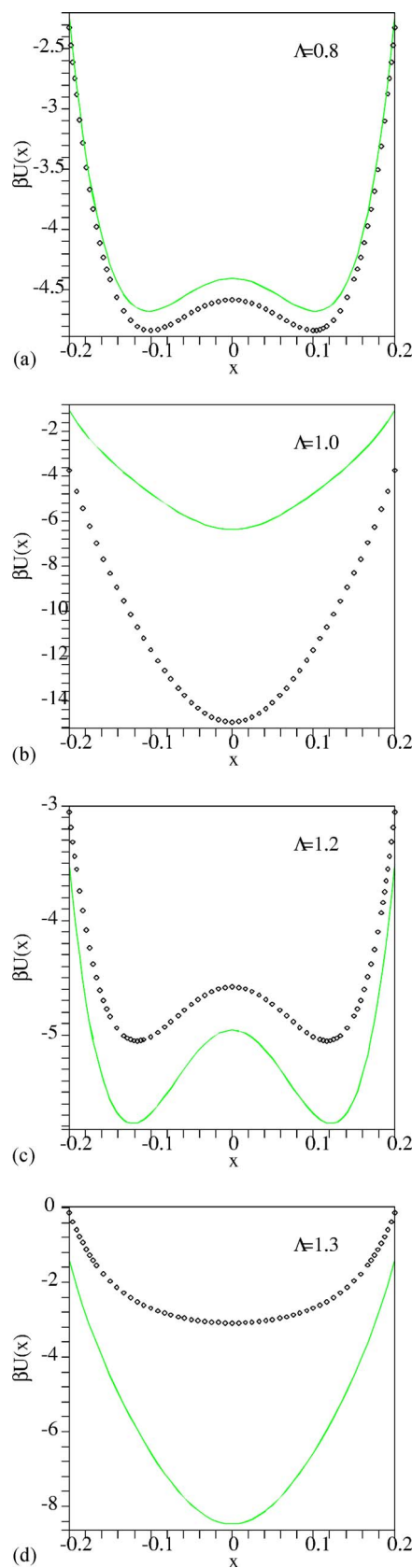


FIG. 10. (Color online) Model 2. Potential experienced by a given particle with neighbors in perfect hexagonal (points) or rectangular (lines) arrangement for different values of Λ .

potential, melts as the value of βV_e is increased. But at stronger external potential, the particles again form a crystalline structure which has rectangular symmetry, similar to what we had observed for the case of model 1. Hence, here also, we observe a reentrant crystallization.

At high external potential strengths, different choices of the parameter Λ need not always result in a rectangular lattice. In Fig. 9 we have plotted the average density for various other values of Λ and $\beta V_e=4.0$. It shows that a rich variety of phases can arise. To understand the structures, we consider the potential energy of a given particle in either triangular or rectangular lattice arrangement. Since both the DLVO and the Gaussian attractive part of the potential fall off rapidly with increasing particle separation, the contribution from the first shell of neighbors is the most significant. Because of the large βV_e , the potential rises sharply in the y direction from the potential troughs. Thus we look for the potential experienced by a particle along the x direction with the y coordinate fixed to be at a minimum of the external potential. Considering the six nearest neighbors for the triangular lattice case and the eight nearest and next-nearest neighbors for the rectangular lattice, we have calculated the effective potential well when all the neighbors are in perfect lattice positions (Fig. 10). For $\Lambda=0.8$, the average density [Fig. 9(a)] looks like a modulated liquid with some superposed modulation perpendicular to the field direction also. Figure 10(a) shows the behavior of the potential well for the same parameter values—both triangular and rectangular lattices are energetically *unstable*. The energy minimum is for a hexagonal arrangement of the neighbors similar to that in triangular lattice, but the central particle has two equivalent energy minima displaced from the center. Thus the system remains frustrated with some residual hexagonal order.

As Λ is tuned to a value of 1.0, a deep minimum in the single particle potential corresponding to a triangular lattice develops [Fig. 10(b)]. However, since we increased Λ through a frustrated potential structure, the system takes a long time to relax to an unique triangular lattice spanning the whole system. Figure 9(c) shows the average density plot for $\Lambda=1.0$. To accommodate the history of the frustrated structure at lower Λ , the shown part of the system goes through a coherent shift along the x direction. At long times, the average density shows sharp contours corresponding to a triangular lattice.

With increasing Λ , the single particle potential with the neighbors in a regular lattice structure again shows degenerate minima, but this time the rectangular lattice wins over the triangular lattice energetically. For $\Lambda=1.2$ the single particle potential is shown in Fig. 10(c) and the corresponding average density contours in Fig. 9(e). The structure is that of a modulated liquid, with superimposed rectangular modulation.

When $\Lambda=1.3$, the rectangular structure is energetically stable and more favored than the triangular lattice [Fig. 10(d)]. The average density plot [Fig. 9(f)] shows sharp contours corresponding to a rectangular structure.

Therefore, once again, we observe that as a function of the location of the minimum of the attractive part of the interparticle potential, the system switches from one kind of crystalline structure (triangular) to another ordered structure (rectangular) via a modulated liquid phase.

IV. CONCLUSIONS

In summary, in this paper we have investigated the effect of an external laser field, periodically modulated in one dimension, on a system of colloidal particles confined to two dimensions and interacting via a potential that includes a short-range attraction component. The presence of this attractive interaction introduces a new length scale (corresponding to the minimum of the attractive pair potential) which can be incommensurate with the wavelength of the potential due to the externally applied laser field. We find that the competition between the two incommensurate length scales results in the phenomenon of *reentrant crystallization* at high field strengths. In both the models we have studied, we find that the crystalline phase attained by the particles at low field strengths melts into a modulated liquid when the strength of the field is increased. However, it eventually crystallizes again, at higher field strengths, due to suppression of the particle motion in the direction of modulation of the applied potential. This phenomenon is opposite to the situation when the attractive interaction is absent, where one observes only reentrant melting. We have also observed, at least in one of the models, that depending upon the position of the minimum of the attractive potential, one can get different phases when both the particle density and the laser potential are kept constant.

We hope that our simulations will motivate experiments to observe the effect of the laser field in two-dimensional colloidal mixtures. Also, in the context of colloidal aggregation, our simulations show that structures with square symmetry in the aggregated phase can be stabilized in the presence of substrates formed by laser intensity fringes. We have also shown that other novel structures can be formed by tuning various parameters of the colloidal system. Further theoretical studies to understand the phenomena observed in our simulations in greater detail would be interesting to pursue.

ACKNOWLEDGMENTS

P.C. would like to thank SERC (IISc) for providing the necessary computation facilities and JNCASR for providing financial support.

- [1] A. Chowdhury, B. J. Ackerson, and N. A. Clark, *Phys. Rev. Lett.* **55**, 833 (1985).
 [2] Q.-H. Wei, C. Bechinger, D. Rudhardt, and P. Leiderer, *Phys. Rev. Lett.* **81**, 2606 (1998).

- [3] J. Chakrabarti, H. R. Krishnamurthy, A. K. Sood, and S. Sengupta, *Phys. Rev. Lett.* **75**, 2232 (1995).
 [4] B. V. Derjaguin and L. D. Landau, *Acta Physicochim. URSS* **14**, 633 (1941); E. J. W. Verwey and J. Th. Overbeek, *Theory*

- of Stability of Lyophobic Colloids* (Elsevier, Amsterdam, 1948).
- [5] C. Das, A. K. Sood, and H. R. Krishnamurthy, *Physica A* **270**, 237 (1999); C. Das, A. K. Sood, and H. R. Krishnamurthy, e-print cond-mat/9902006.
- [6] J. M. Kosterlitz and D. J. Thouless, *J. Phys. C* **6**, 1181 (1978); B. I. Halperin and D. R. Nelson, *Phys. Rev. Lett.* **41**, 121 (1978); A. P. Young, *Phys. Rev. B* **19**, 1855 (1979); D. R. Nelson, in *Phase Transitions and Critical Phenomena*, edited by C. Domb and J. Lebowitz (Academic, New York, 1983), Vol. 7, p. 1.
- [7] E. Frey, D. R. Nelson, and L. Radzihovsky, *Phys. Rev. Lett.* **83**, 2977 (1999); L. Radzihovsky, E. Frey, and D. R. Nelson, *Phys. Rev. E* **63**, 031503 (2001).
- [8] C. Bechinger, M. Brunner, and P. Leiderer, *Phys. Rev. Lett.* **86**, 930 (2001).
- [9] W. Strepp, S. Sengupta, and P. Nielaba, *Phys. Rev. E* **66**, 056109 (2002); D. Chaudhuri and S. Sengupta, e-print cond-mat/0508514.
- [10] C. Das, P. Chaudhuri, A. Sood, and H. Krishnamurthy, *Curr. Sci.* **80**, 959 (2001).
- [11] W. Strepp, S. Sengupta, and P. Nielaba, *Phys. Rev. E* **63**, 046106 (2001); D. Chaudhuri and S. Sengupta, *Europhys. Lett.* **67**, 814 (2004).
- [12] J. Baumgartl, M. Brunner, and C. Bechinger, *Phys. Rev. Lett.* **93**, 168301 (2004).
- [13] S. Asakura and F. Oosawa, *J. Polym. Sci.* **33**, 183 (1958).
- [14] G. M. Kepler and S. Fraden, *Phys. Rev. Lett.* **73**, 356 (1994).
- [15] D. G. Grier, *Nature (London)* **393**, 621 (1998); J. C. Crocker and D. G. Grier, *Phys. Rev. Lett.* **77**, 1897 (1996).
- [16] In a recent paper, [J. Baumgartl and C. Bechinger, *Europhys. Lett.* **71**, 487 (2005)], it has been suggested that the conclusion about the attractive effective potential near the wall is an artifact of the way particle positions are measured through microscopes, because, at short distances, identifying particle positions through intensity maxima gives wrong results unless a superposition of intensity from both the particles is taken in account. The claim of this paper is that if the latter is done, then the deduced interaction potential goes back to a DLVO-like, purely repulsive, form.
- [17] I. O. Götze, J. M. Brader, M. Schmidt, and H. Lowen, *Mol. Phys.* **101**, 1651 (2003).
- [18] R. Castaneda-Priego, A. Rodriguez-Lopez, and J. M. Mendez-Alcaraz, *J. Phys.: Condens. Matter* **15**, S3393 (2003).
- [19] J. J. Cerda, T. Sintes, C. M. Sorensen, and A. Chakrabarti, *Phys. Rev. E* **70**, 011405 (2004).
- [20] P. Bolhuis, M. Hagen, and D. Frenkel, *Phys. Rev. E* **50**, 4880 (1994).
- [21] V. J. Anderson and H. W. Lekkerkerker, *Nature (London)* **416**, 811 (2002).